JOURNAL OF COMPUTATIONAL PHYSICS 81, 206–229 (1989)

Application of Spectral Collocation Techniques to the Stability of Swirling Flows

MEHDI R. KHORRAMI

Department of Mechanical Engineering and Mechanics, Old Dominion University, Norfolk, Virginia 23529-0247

MUJEEB R. MALIK

High Technology Corporation, P.O. Box 7262, Hampton, Virginia 23666

AND

ROBERT L. ASH

Department of Mechanical Engineering and Mechanics, Old Dominion University, Norfolk, Virginia 23529-0247

Received September 28, 1987; revised May 6, 1988

A Chebyshev spectral collocation method for the temporal and spatial stability of swirling flows is presented. The linearized stability equations in cylindrical coordinates are solved using the method and eigenvalues obtained by employing the QZ routine. The developed algorithm is found to be robust and easily adaptable to various flow configurations, including internal and external flows, with only minor changes in the application of the boundary conditions. The accuracy and efficiency of the spectral method is tested for plane Poiseuille flow, annular flow, rotating pipe flow, and a trailing line vortex. © 1989 Academic Press, Inc.

1. INTRODUCTION

The applicability of Chebyshev spectral methods for solving hydrodynamic stability problems was first demonstrated by Orszag [1]. Subsequent applications of the technique to similar boundary value problems have further brought out the high degree of accuracy achievable using spectral methods, (Metcalfe and Orszag [2], Zebib [3], and Bridges and Morris [4]). However, of the three distinct Chebyshev formulations (Galerkin, tau, and collocation), the cited stability calculations have employed only the Galerkin or the tau approach.

Howard and Gupta [5] have shown that no general necessary and sufficient condition can be developed for delineating the stability of vortex flows subjected to asymmetric disturbances. Consequently, a separate stability analysis is required for

0021-9991/89 $3.00

each type of vortex flow. This precludes then the Galerkin or the tau method as the most attractive approach to obtain the eigenvalues, since major modifications may be required when the mean velocity profile is changed or a new coordinate transformation is involved. This is due to the fact that for both the tau and Galerkin methods the operators for the governing equations are always evaluated in the Chebyshev space, and thus must be modified for changes in the flow description.

For the vortex stability problem, a spectral collocation method appears more attractive since a computational algorithm based on that method does not require major modifications from case to case and at the same time the computations are accurate and efficient. Therefore, a spectral collocation formulation of the linearized equations of motion for a steady, 3-dimensional, constant density fluid flow has been developed. The formulation is described in the subsequent sections. Although the spectral collocation technique has been applied to the Orr–Sommerfeld equation (Herbert [6], Spalart [7]), there appears to be no previous application of the method to the type of problems discussed in this paper.

A Chebyshev collocation matrix algorithm has been constructed for both spatial and temporal stability calculations. In the present method, the derivatives of the eigenfunctions are evaluated in the physical space at the collocation points. Through numerous test cases which examined annular flow (including the narrow gap limit of plane Poiseuille flow), cylindrical Poiseuille flow, rotating pipe flow, and a trailing line vortex, we have shown that the developed algorithm produces accurate global eigenvalues for each case without requiring any substantial changes in the computer code.

A future goal of this research will be to perform stability analyses of the similarity solutions for porous rotating pipe flow obtained by Donaldson and Sullivan [8]. Their computed profiles which are exact solutions to the 3-dimensional equations of motion have shown many of the flow features which are of interest in the study of unconfined trailing line vortices. For example, their solutions range from those which can be characterized as a single cell vortex to multiple cell vortices. In addition, experimental measurements have documented the existance of many of these flows (see Adams and Gilmore [9], Leuchter and Solignac [10], and Graham and Newman [11]). However, this study has been concerned primarily with validation of the spectral collocation method and to that end, the algorithm has been studied for some classical velocity profiles for which some stability results are available.

2. Problem Formulation

We consider cylindrical-polar coordinates (r, θ, z) in which the governing equations of motion are written as:

continuity

$$\frac{1}{r}\frac{\partial}{\partial r}(ru') + \frac{1}{r}\frac{\partial v'}{\partial \theta} + \frac{\partial w'}{\partial z} = 0 \tag{1}$$

r-momentum

$$\frac{\partial u'}{\partial t}+u'\frac{\partial u'}{\partial r}+\frac{v'}{r}\frac{\partial u'}{\partial \theta}+w'\frac{\partial u'}{\partial z}-\frac{v'^2}{r}$$
$$=-\frac{1}{\rho}\frac{\partial p'}{\partial r}+\nu\left(\nabla^2 u'-\frac{u'}{r^2}-\frac{2}{r^2}\frac{\partial v'}{\partial \theta}\right) \tag{2}$$

θ-momentum

$$\frac{\partial v'}{\partial t}+u'\frac{\partial v'}{\partial r}+\frac{v'}{r}\frac{\partial v'}{\partial \theta}+w'\frac{\partial v'}{\partial z}+\frac{u'v'}{r}$$
$$=-\frac{1}{\rho r}\frac{\partial p'}{\partial \theta}+\nu\left(\nabla^2 v'-\frac{v'}{r^2}+\frac{2}{r^2}\frac{\partial u'}{\partial \theta}\right) \tag{3}$$

z-momentum

$$\frac{\partial w'}{\partial t}+u'\frac{\partial w'}{\partial r}+\frac{v'}{r}\frac{\partial w'}{\partial \theta}+w'\frac{\partial w'}{\partial z}=-\frac{1}{\rho}\frac{\partial p'}{\partial z}+\nu\nabla^2 w', \tag{4}$$

where

$$\nabla^2\equiv\frac{\partial^2}{\partial r^2}+\frac{1}{r}\frac{\partial}{\partial r}+\frac{1}{r^2}\frac{\partial^2}{\partial \theta^2}+\frac{\partial^2}{\partial z^2}.$$

The flow variables are assumed to consist of a mean part and an infinitesimally small perturbation, i.e.,

$$\begin{aligned} u' &= U+u \\ v' &= V+v \\ w' &= W+w \\ p' &= \Pi+p. \end{aligned} \tag{5}$$

Following Donaldson and Sullivan [8], the basic flow is assumed to be of the form:

$$\begin{aligned} U &= U(r) \\ V &= V(r) \\ W &= z\bar{W}(r), \end{aligned} \tag{6}$$

where U, V, and W are the radial, tangential, and axial velocities, respectively. The z-dependence of the axial velocity, W, indicated above is treated using a quasi-parallel flow approximation. The approximation can be justified on dimensional

grounds using arguments similar to those employed by Donaldson and Sullivan in their similarity analysis. Assuming that the axial (z) coordinate has been made dimensionless by tube radius, R_0, and using a Reynolds number, Re, based on tube radius, the axial velocity can be represented as

$$W(r, z) = 4C \frac{z}{\mathrm{Re}} f'(\eta) \tag{7}$$

where η is a similarity variable for the radial coordinate and C is a nondimensional pressure gradient.

The maximum value for $f'(\eta)$ in (7) is unity. Consequently, if z is chosen as

$$z_0 = \mathrm{Re}/4C, \tag{8}$$

then

$$W(r, z_0) = f'(\eta). \tag{9}$$

At z_0, the axial gradient of $W(r, z)$ is given by

$$\frac{\partial W}{\partial z}(r, z_0) = \frac{4C}{\mathrm{Re}} f'(\eta) = \psi \tag{10}$$

which is very small since flows of interest have high Reynolds numbers. The quasi-parallel flow assumption is therefore justified. For cases where z is small or where pressure gradient rather than viscous forces are responsible for the z-dependence, one can use a multiple-scale analysis to account for nonparallel effects. The spectral collocation method developed in the present study can be used for such an analysis. However, we have assumed a "quasi-parallel" basic flow here and the disturbance quantities are assumed to have the form:

$$\{u, v, w, p\} = \{iF(r), G(r), H(r), P(r)\}\, e^{i(\alpha z + n\theta - \omega t)}. \tag{11}$$

Here, F, G, H, and P are the disturbances eigenfunctions, α is the wavenumber in the axial direction, n is the wavenumber in the azimuthal direction, and ω is the temporal frequency. For a single-valued solution, n must be an integer or zero. For n equal to zero, axisymmetric disturbances exist. When n is a positive or negative integer, asymmetric disturbances occur which represent different directions of propagation, depending on the sign of n/ω.

If spatial stability is considered, then ω is real and $\alpha = \alpha_r + i\alpha_i$. On the other hand for a temporal solution, α is real and $\omega = \omega_r + i\omega_i$. In either case, the sign of the imaginary part indicates decay or growth of the disturbance.

Substituting (5) and (11) into the governing equations (1)–(4) and neglecting the nonlinear terms, the linearized form of the equations is obtained. They can be written in nondimensional form:

continuity

$$F' + \frac{F}{r} + \frac{nG}{r} + \alpha H = 0 \tag{12}$$

r-momentum

$$-\frac{iF''}{\mathrm{Re}} + i\left[U - \frac{1}{\mathrm{Re}\, r}\right]F' + \left[\omega + i\frac{dU}{dr} - \frac{nV}{r} - \alpha W + \frac{i}{\mathrm{Re}}\left(\frac{n^2+1}{r^2} + \alpha^2\right)\right]F + \left[\frac{i2n}{\mathrm{Re}\, r^2} - \frac{2V}{r}\right]G + P' = 0 \tag{13}$$

θ-momentum

$$-\frac{G''}{\mathrm{Re}} + \left[U - \frac{1}{\mathrm{Re}\, r}\right]G' + \left[-i\omega + \frac{inV}{r} + i\alpha W + \frac{U}{r} + \frac{1}{\mathrm{Re}}\left(\frac{n^2+1}{r^2} + \alpha^2\right)\right]G + \left[i\frac{dV}{dr} + \frac{2n}{\mathrm{Re}\, r^2} + \frac{iV}{r}\right]F + \frac{inP}{r} = 0 \tag{14}$$

z-momentum

$$-\frac{H''}{\mathrm{Re}} + \left[U - \frac{1}{\mathrm{Re}\, r}\right]H' + \left[-i\omega + \frac{inV}{r} + i\alpha W + \psi + \frac{1}{\mathrm{Re}}\left(\frac{n^2}{r^2} + \alpha^2\right)\right]H + i\frac{\partial W}{\partial r}F + i\alpha P = 0. \tag{15}$$

Where Re is the Reynolds number based on pipe radius, R_0, and primes denote differentiation with respect to the radial coordinate. At the outer wall the no-slip condition is enforced for all velocities. Due to the singular nature of the coordinate system and because all physical quantities must be smooth and bounded on the centerline, some non-trivial requirements exist as $r \to 0$. That is, on the centerline

$$\lim_{r\to 0} \frac{\partial \mathbf{V}}{\partial \theta} = 0$$
$$\lim_{r\to 0} \frac{\partial p'}{\partial \theta} = 0, \tag{16}$$

where $\mathbf{V}$ is the total velocity vector. These limits (16) represent boundedness and smoothness conditions on the solutions along the centerline. The relations (16) are the formalized form of the compatibility relations given previously by Batchelor and Gill [12]. In expanding the conditions (16), we need to consider only the perturbation part of the velocity since the mean flow is independent of the azimuthal direction. Representing the perturbation velocity field by $\mathbf{v}$, we have

$$\frac{\partial \mathbf{v}}{\partial \theta} = \frac{\partial}{\partial \theta}(u\mathbf{e}_r + v\mathbf{e}_\theta + w\mathbf{e}_z)$$

or

$$\lim_{r\to 0}\frac{\partial \mathbf{v}}{\partial\theta}=\frac{\partial u}{\partial\theta}\mathbf{e}_r+u\frac{d\mathbf{e}_r}{d\theta}+\frac{\partial v}{\partial\theta}\mathbf{e}_\theta+v\frac{d\mathbf{e}_\theta}{d\theta}+\frac{\partial w}{\partial\theta}\mathbf{e}_z+w\frac{d\mathbf{e}_z}{d\theta}.$$

But

$$\frac{d\mathbf{e}_z}{d\theta}=0$$

$$\frac{d\mathbf{e}_r}{d\theta}=\mathbf{e}_\theta$$

$$\frac{d\mathbf{e}_\theta}{d\theta}=-\mathbf{e}_r;$$

substituting from (11), we deduce

$$\lim_{r\to 0}\frac{\partial \mathbf{v}}{\partial\theta}=(-nF-G)\,\mathbf{e}_r+(iF+inG)\,\mathbf{e}_\theta+inH\mathbf{e}_z=0.$$

In order for the equality to hold, each component of the resultant vector must be zero. Similarly, application of the limit process to the perturbation pressure field yields

$$\lim_{r\to 0}\frac{\partial p}{\partial\theta}=inP=0.$$

Summarizing, in the limit along the centerline ($r=0$), we have

$$\begin{aligned} nF+G&=0\\ F+nG&=0\\ nH&=0\\ nP&=0. \end{aligned}\tag{16a}$$

The above conditions depend on the value of the azimuthal wavenumber, n, such that if $n=0$,

$$\begin{aligned} &F(0)=G(0)=0\\ &H(0)\text{ and }P(0)\text{ must be finite;} \end{aligned}\tag{17}$$

if $n=\pm 1$,

$$\begin{aligned} &F(0)\pm G(0)=0\\ &H(0)=P(0)=0; \end{aligned}\tag{18}$$

or if $|n| > 1$,

$$F(0) = G(0) = 0$$
$$H(0) = P(0) = 0. \tag{19}$$

In the case when $|n| = 1$, two of the conditions become linearly dependent. Another relation was deduced by enforcing the continuity equation on the centerline. Since $H(0) = 0$,

$$\lim_{r \to 0} \left[F' + \frac{1}{r}(F + nG) + \alpha H \right] = 2F'(0) + nG'(0) = 0. \tag{20}$$

2.1. *Spectral Collocation Technique*

A Chebyshev collocation approach was chosen for this study. The use of collocation simplifies the treatment of various boundary conditions and coordinate transformations considerably. The implementation of the resulting algorithm is also straightforward. Furthermore, Chebyshev polynomials distribute the error evenly, exhibit rapid convergence rates with increasing numbers of terms, and cluster the collocation points near the boundaries [13–15].

Chebyshev polynomials are defined on the interval $(-1, 1)$ by

$$T_k(\xi) = \cos[k \cos^{-1} \xi]. \tag{21}$$

Because the physical range in this problem is $(0, 1)$, a simple transformation is made from the physical variable r to the Chebyshev variable ξ via

$$\xi = 1 - 2r, \tag{22}$$

where

$$-1 \leqslant \xi \leqslant 1.$$

If,

$$\xi = \cos \phi,$$

it can be seen that (21) becomes

$$T_k(\xi) = \cos k\phi. \tag{23}$$

The collocation points which are the extrema of the last retained Chebyshev polynomial in the truncated series are defined by

$$\xi_j = \cos \frac{\pi j}{N}, \qquad j = 0, 1, ..., N, \tag{24}$$

where the centerline and outer wall boundaries, correspond to j equals 0 and N, respectively.

An interpolant polynomial is constructed in terms of the values of the flow variable at the collocation points by employing a truncated Chebyshev series. Next, the first and second derivatives of the variable are determined explicitly using the above interpolant. As an example, we present expressions for $F(\xi)$, since extension to the other variables is straightforward. If $F(\xi)$ is represented by

$$F(\xi) = \sum_{k=0}^{N} a_k T_k(\xi),$$

then

$$\left.\frac{dF}{d\xi}\right|_j = \sum_{k=0}^{N} A_{jk} F_k \tag{25}$$

$$\left.\frac{d^2F}{d\xi^2}\right|_j = \sum_{k=0}^{N} B_{jk} F_k \tag{26}$$

$j = 0, 1, ..., N$, where A_{jk} and B_{jk} are the elements of the derivative matrices and are given [15] as

$$A_{jk} = \frac{\bar{C}_j}{\bar{C}_k} \frac{(-1)^{k+j}}{\xi_j - \xi_k} \qquad (j \neq k) \tag{27}$$

$$A_{jj} = -\frac{\xi_j}{2(1-\xi_j^2)}$$

$$A_{00} = \frac{2N^2+1}{6} = -A_{NN}$$

with

$$\bar{C}_0 = \bar{C}_N = 2, \qquad \bar{C}_j = 1, \qquad (1 \leqslant j \leqslant N-1)$$

and

$$B_{jk} = A_{jm} A_{mk}. \tag{28}$$

Note that any higher derivative can be obtained by employing relation (28).

Writing Eqs. (12)–(15) in terms of the Chebyshev variable and evaluating at the collocation points yields

continuity

$$S_1 \sum_{k=0}^{N} A_{jk} F_k + \left(\frac{2}{1-\xi_j}\right) F_j + \left(\frac{2n}{1-\xi_j}\right) G_j + \alpha H_j = 0 \tag{29}$$

r-momentum

$$S_2 \sum_{k=0}^{N} B_{jk} F_k + \left[\frac{2}{1-\xi_j} - \mathrm{Re}\, U_j \right] S_1 \sum_{k=0}^{N} A_{jk} F_k + \left[i\,\mathrm{Re}\,\omega - \mathrm{Re}\, S_1 \frac{dU}{d\xi}\bigg|_j - \frac{i2\,\mathrm{Re}\, nV_j}{1-\xi_j} - \left(\frac{4(n^2+1)}{(1-\xi_j)^2} \right) \right] F_j - \left[\frac{4(2n)}{(1-\xi_j)^2} + \frac{2(i2\,\mathrm{Re}\, V_j)}{1-\xi_j} \right] G_j + i\,\mathrm{Re}\, S_1 \sum_{k=0}^{N} A_{jk} P_k - i\alpha\,\mathrm{Re} W_j F_j - \alpha^2 F_j = 0 \tag{30}$$

θ-momentum

$$- \left[i\,\mathrm{Re}\, S_1 \frac{dV}{d\xi}\bigg|_j + \frac{4(2n)}{(1-\xi_j)^2} + \frac{2(i\,\mathrm{Re}\, V_j)}{(1-\xi_j)} \right] F_j + S_2 \sum_{k=0}^{N} B_{jk} G_k + \left[\frac{2}{1-\xi_j} - \mathrm{Re}\, U_j \right] S_1 \sum_{k=0}^{N} A_{jk} G_k + \left[i\,\mathrm{Re}\,\omega - \frac{2(i\,\mathrm{Re}\, nV_j)}{1-\xi_j} - \frac{2(\mathrm{Re}\, U_j)}{1-\xi_j} - \frac{4(n^2+1)}{(1-\xi_j)^2} \right] G_j - \frac{2(i\,\mathrm{Re}\, n)}{1-\xi_j} P_j - i\alpha\,\mathrm{Re}\, W_j G_j - \alpha^2 G_j = 0 \tag{31}$$

z-momentum

$$- i\,\mathrm{Re}\, S_1 \frac{\partial W}{\partial \xi}\bigg|_j F_j + S_2 \sum_{k=0}^{N} B_{jk} H_k + \left[\frac{2}{1-\xi_j} - \mathrm{Re}\, U_j \right] S_1 \sum_{k=0}^{N} A_{jk} H_k + \left[i\,\mathrm{Re}\,\omega - \frac{2(i\,\mathrm{Re}\, nV_j)}{1-\xi_j} - \mathrm{Re}\,\psi_j - \frac{4n^2}{(1-\xi_j)^2} \right] H_j - i\alpha\,\mathrm{Re}\, W_j H_j - i\alpha\,\mathrm{Re}\, P_j - \alpha^2 H_j = 0. \tag{32}$$

Here S_1 and S_2 are first and second derivative scaling factors developed from the coordinate transformation. The boundary conditions are, at $\xi = -1$,

$$F(-1) = G(-1) = H(-1) = 0$$

and

$$\frac{\partial P}{\partial r}\bigg|_{\xi=-1} = \chi, \qquad \text{for all } n. \tag{33}$$

At $\xi = 1$, if $n = 0$,

$$\begin{aligned} &F(1) = G(1) = 0 \\ &H(1) \text{ and } P(1) \text{ are finite;} \end{aligned} \tag{34}$$

if $n = \pm 1$,

$$\begin{aligned} F(1) \pm G(1) &= 0 \\ H(1) = P(1) &= 0 \\ 2F'(1) \pm G'(1) &= 0; \end{aligned} \tag{35}$$

or if $|n| > 1$,

$$\begin{aligned} F(1) = G(1) &= 0 \\ H(1) = P(1) &= 0. \end{aligned} \tag{36}$$

The pressure boundary condition (33) and its effect on numerical calculations will be discussed later.

2.2. *Numerical Scheme*

Originally, the iterative method of Bridges and Morris [4] was selected to obtain the spatial solution. However, soon it was realized that the leading coefficient matrix (that is coefficients containing an α^2 term) in this problem is non-monic and singular [4]. Bridges and Morris [4] have indicated that for this type of leading matrix, the convergence behavior of the iterative scheme is unknown at the present time. Therefore, a companion matrix method was selected to perform spatial calculations. This is a standard method in which the quadratic terms in α are linearized with a simple transformation. That is, for the spatial formulation, three new variables, $\bar{F}$, $\bar{G}$, $\bar{H}$ are defined:

$$\begin{aligned} \bar{F}_j &= \alpha F_j \\ \bar{G}_j &= \alpha G_j \\ \bar{H}_j &= \alpha H_j. \end{aligned} \tag{37}$$

The extra boundary conditions on $\bar{F}$, $\bar{G}$, and $\bar{H}$ are identical to the conditions (33)–(36) without the pressure condition.

The above governing equations can be represented in the generalized eigenvalue format as

$$D\mathbf{X} = \lambda E\,\mathbf{X}. \tag{38}$$

For the case of spatial stability,

$$\lambda = \alpha$$

and

$$\mathbf{X} = [F\ G\ H\ P\ \bar{F}\ \bar{G}\ \bar{H}]^{\mathrm{T}}. \tag{39}$$

For the temporal case,

$$\lambda = \omega$$

and

$$\mathbf{X} = [F\ G\ H\ P]^{\mathrm{T}}. \tag{40}$$

Both D and E are square matrices with dimensions of $7(N+1)$ or $4(N+1)$. Depending on the spatial or temporal stability, the last 14 or 8 rows of matrix D contain the boundary conditions. Since the boundary conditions do not contain the eigenvalue λ, the submatrix in D containing these conditions was made upper triangular through column operations. If all of the diagonal elements of this submatrix are non-zero, it indicates that the boundary conditions are independent of each other and the ranks of matrices D and E are reduced to $7(N-1)$ or $4(N-1)$.

It should be noted that the eigenvalue coefficient matrix, E, is singular. A procedure may be devised using row and column operations which reduces the rank of the coefficient matrix and removes the singularity (see, e.g., Metcalfe and Orszag [2]). Such a procedure was implemented in our work. An alternative approach is to introduce a term $\gamma\omega P_j$ in the temporal formulation of the continuity equation (29). This additional term makes the coefficient matrix for ω non-singular and may be termed an artificial compressibility factor (see Malik and Poll [16]). It was found that computations using the method of artificial compressibility of Malik and Poll were at least one-and-a-half times faster than the matrix operations of Metcalf and Orszag [2], and both produced identical eigenvalues. For the spatial case, the term $\gamma\alpha\bar{H}_j$ was added to Eq. (29), when the artificial compressibility method was used, to remove the singularity. The parameter γ was assigned a very small value. This term generated large values for some of the eigenvalues of the matrix $E^{-1}D$; however, experimentation with the value of γ demonstrated that its effect on the desired (physical) eigenvalues was negligible.

Before investigating a range of mean velocity profiles from [8], it was decided to test the versatility of the algorithm against model problems where solutions already exist. Each model solution will be discussed individually in some detail in the next section. All of the numerical solutions were obtained on the CDC CYBER 860 machines at NASA Langley Research Center. Occasionally, when larger matrices were involved, solutions were obtained using a CDC VPS 32 machine. The generalized complex eigenvalue solver employed was the IMSL QZ routine called EIGZC.

3. Test Cases

The problems presented in this section were selected to represent the variety of flow domains and boundary conditions which could be studied with the spectral collocation code. The primary goal was to use these sample calculations to demonstrate the accuracy and efficiency of the present formulation, rather than to attempt to duplicate the earlier works of others.

3.1. *Spatial Stability of Flow through a Narrow Gap Annulus*

In the narrow gap limit, the spectrum of eigenvalues for axisymmetric disturbances approach those obtained for the Orr–Sommerfeld equation for plane Poiseuille flow. Here, the mean velocity profile for an annulus is of the form

$$\begin{aligned} U &= 0 \\ V &= 0 \\ W &= \frac{1 - r^2 + r_M^2 \ln r^2}{1 - r_M^2 + r_M^2 \ln r_M^2}, \end{aligned} \tag{41}$$

where non-dimensionalization is with respect to the maximum velocity and the half gap distance and r_M is the location of maximum velocity. For this problem, we use the transformation

$$\xi = 1 - r + \frac{2R_i}{(R_0 - R_i)}, \tag{42}$$

where

$$\frac{2R_i}{(R_0 - R_i)} \leqslant r \leqslant \frac{2R_0}{(R_0 - R_i)}.$$

R_i and R_0 are the inner and outer radii, respectively. The no-slip boundary conditions are imposed at the two solid walls. That is,

$$\begin{aligned} F(1) = G(1) = H(1) &= 0 \\ \bar{F}(1) = \bar{G}(1) = \bar{H}(1) &= 0 \\ \left.\frac{\partial P}{\partial r}\right|_{\xi = 1} &= \chi \end{aligned} \tag{43}$$

and

$$\begin{aligned} F(-1) = G(-1) = H(-1) &= 0 \\ \bar{F}(-1) = \bar{G}(-1) = \bar{H}(-1) &= 0 \\ \left.\frac{\partial P}{\partial r}\right|_{\xi = -1} &= \chi. \end{aligned} \tag{44}$$

The type of Neumann conditions specified for pressure is a well-known procedure whenever the Navier–Stokes equations are being solved in the primitive variables. This issue has been discussed by Orszag and Israeli [17]. The value of χ is prescribed by taking the inner product of the momentum equation with the boundary normal direction. In the cylindrical-polar coordinates this turns out to be the r-momentum equation in its original form evaluated at the boundaries.

The two artificial pressure conditions in (43) and (44) may be altogether avoided by staggering the pressure terms and the continuity equation. This is accomplished by representing the pressure with a polynomial of $N-1$ (rather than N) degree. At the same time a set of interpolating matrices must be developed to interpolate from the staggered points to the cell faces and vice versa. This procedure is quite involved and its programming is not as straightforward. We are currently working on this aspect of the problem; however, we will show in subsequent sections that pressure conditions (43) and (44) not only are viable but also produce accurate results with a substantial reduction in the complexity of the coding.

Employing the tau formulation and even Chebyshev polynomials, Bridges and Morris [4] have reported on the critical wave number for the plane Poiseuille flow. Their results, along with the present calculations, are tabulated in Table I. To the degree of accuracy given by both methods, the critical wavenumbers are almost identical, agreeing in the sixth or seventh digits. Table II shows the eigenvalue spectrum for plane Poiseuille flow obtained by Bridges and Morris [4] and those of the present calculations. Again, the eigenvalues match up to the fifth or sixth decimal place. For the case $N+1=62$, due to the large size of the matrices, round off error starts to show up in the unstable mode. However, this error is negligible and there has been no need to go to such high polynomial order.

3.2. *Temporal Stability of Narrow Gap Annulus*

An accurate set of eigenvalues for plane Poiseuille flow has been reported by Orszag [1], where the Chebyshev tau method has been used. He divided the eigenvalues into sets of symmetric and antisymmetric modes where the former set was obtained using an even Chebyshev series while the latter set was found using an odd series. Ten of these modes were obtained by the present calculations and are

TABLE I

Comparison of the Result of Bridges and Morris with That Obtained by Chebyshev Collocation

Bridges and Morris [4]		Present method	
$N+1$	α	$N+1$	α
32	$1.020556+i9.74(-07)$	42	$1.020557+i8.13(-07)$

Note. $\mathrm{Re}=5772$, $\omega=0.26943$.

TABLE II

Comparison of the Eigenvalue Spectrum for Spatial Stability of Plane Poiseuille Flow due to Bridges and Morris with Those Obtained by Chebyshev Collocation

Mode	Bridges and Moris [4]	Present Method	
		$N+1=42$	$N+1=62$
1	$1.00047 - i0.00086$	$1.000473 - i0.000863$	$1.000468 - i0.000872$
2	$0.28323 + i0.02538$	$0.283232 + i0.025381$	$0.283232 + i0.025381$
4	$0.31976 + i0.07532$	$0.319763 + i0.075318$	$0.319763 + i0.075318$
5	$0.33745 + i0.10492$	$0.33744 + i0.1049$	$0.337449 + i0.104920$
6	$0.35456 + i0.13782$	$0.35 + i0.137$	$0.354564 + i0.137823$
7	$0.37090 + i0.17425$		$0.370905 + i0.174246$
8	$0.38629 + i0.21480$		$0.386286 + i0.214801$
9	$0.40156 + i0.26063$		$0.401555 + i0.260635$
10	$0.42050 + i0.31175$		$0.420492 + i0.311771$

Note. $\mathrm{Re} = 6000$, $\omega = 0.26$.

tabulated in Table III along with those of Orszag [1]. The agreement between the two calculations is excellent for the first few modes but deteriorates for the rest of the eigenvalues. This lack of agreement is due to the fact that ordering of eigenvalues for the present calculation was done for the sake of comparison. The actual computed eigenvalue spectrum contains many converged lower stable modes which are unique to the Poiseuille flow in an annulus and therefore are not reported here. As a next step, the gap width was reduced further while keeping N, the order of Chebyshev polynomials, fixed. The eigenvalues given in Table III were found to move and converge towards those reported by Orszag [1].

TABLE III

Least Stable Eigenvalues for $\alpha = 1$, $\mathrm{Re} = 10000$

Mode	Orszag [1]	Present method
1	$0.23752649 + 0.00373967i$	$0.2375267 + 0.0037398i$
2	$0.96463092 - 0.03516728i$	$0.9646309 - 0.0315672i$
3	$0.96464251 - 0.03518658i$	$0.9646425 - 0.0351865i$
4	$0.27720434 - 0.05089873i$	$0.2772045 - 0.0508986i$
5	$0.93631654 - 0.06320150i$	$0.936316 - 0.063201i$
6	$0.93635178 - 0.06325157i$	$0.936351 - 0.063251i$
7	$0.90798305 - 0.09122274i$	$0.90798 - 0.09122i$
8	$0.90805633 - 0.09131286i$	$0.90805 - 0.09131i$
9	$0.87962729 - 0.11923285i$	$0.8796 - 0.1192i$
10	$0.87975570 - 0.11937073i$	$0.8797 - 0.1193i$

3.3. *Spatial Stability of Poiseuille Flow in a Pipe*

The mean velocity for this problem is the well-known profile given by

$$\begin{aligned} U &= 0 \\ V &= 0 \\ W &= 1 - r^2, \end{aligned} \tag{45}$$

and the boundary conditions are

at $\xi = -1$, for all n

$$\begin{aligned} &F(-1) = G(-1) = H(-1) = 0 \\ &\bar{F}(-1) = \bar{G}(-1) = \bar{H}(-1) = 0 \\ &\left.\frac{\partial P}{\partial r}\right|_{\xi=-1} = \chi \end{aligned} \tag{46}$$

at $\xi = 1$

$$\begin{aligned} &F(1) = G(1) = \bar{F}(1) = \bar{G}(1) = 0 \\ \text{if } n = 0 \quad &\left.\frac{\partial H}{\partial r}\right|_{\xi=1} = \left.\frac{\partial \bar{H}}{\partial r}\right|_{\xi=1} = 0 \\ &\left.\frac{\partial P}{\partial r}\right|_{\xi=1} = \chi \end{aligned} \tag{47}$$

$$\begin{aligned} &H(1) = \bar{H}(1) = P(1) = 0 \\ &F(1) + nG(1) = 0 \\ \text{if } n = \pm 1 \quad &\bar{F}(1) + n\bar{G}(1) = 0 \\ &2F'(1) + nG'(1) = 0 \\ &2\bar{F}'(1) + n\bar{G}'(1) = 0 \end{aligned} \tag{48}$$

or

$$\begin{aligned} &F(1) = \bar{F}(1) = G(1) = \bar{G}(1) = 0 \\ \text{if } |n| > 1 \quad &H(1) = \bar{H}(1) = P(1) = 0. \end{aligned} \tag{49}$$

The boundary conditions (46)–(49), minus the terms with bar superscript which are particular to the spatial formulation, are the conditions employed for the rest of the cases used in this study and therefore will not be repeated for each individual case.

TABLE IV

Comparison of the Result of Garg and Rouleau with That Obtained by Chebyshev Collocation

	Garg and Rouleau [18]	Present method
n	α	α
0	$0.51998925173 + 0.02083549388i$	$0.51998925171 + 0.02083549388i$
1	$0.5352510831 + 0.0172276439i$	$0.53525108 + 0.01722763i$

Note. $\mathrm{Re} = 10000$, $\omega = 0.5$.

The spatial stability of Poiseuille flow in a pipe has been reported by Garg and Rouleau [18]. Starting with a series solution near the centerline of the pipe, they integrated the governing equations employing a fourth-order Runge–Kutta scheme. For each particular set of parameters Re, ω, and n, a single eigenvalue was obtained through iteration until the boundary conditions at the outer wall were satisfied. Using a very small integration step size of 0.001, they obtained eigenvalues which were claimed to be accurate to at least nine significant digits. Two of their modes, along with the present results (using $N = 40$), are listed in Table IV. For the axisymmetric case (where $n = 0$) the agreement is excellent and the two values agree to 10 or 11 digits. However, the agreement is not as good for $n = 1$ as for $n = 0$; and as has been pointed out by [18], the loss of accuracy is caused by the twofold increase in the number of calculations for $n = 1$. As a test for the convergence and accuracy of the collocation method, the number of the collocation points, N was increased gradually and the convergence of the eigenvalues was observed. The result for $n = 0$ is tabulated in Table V and shows that for moderate values of N, six-digit accuracy is obtained.

As a check on any effect of round off errors and on the value of the artificial compressibility parameter, the same set of eigenvalues was calculated with $\gamma = 10^{-12}$

TABLE V

The Convergence Property of the Chebyshev Collocation Method

N	α_r	α_i
20	0.519991235	0.020832533
21	0.519988229	0.020836174
22	0.519989641	0.020835397
23	0.519989125	0.020835487
30	0.519989251710	0.020835493892
40	0.519989251713	0.020835493884

Note. $\mathrm{Re} = 10000$, $\omega = 0.5$. and $n = 0$. N is the number of Chebyshev terms used to represent each of the flow variables.

TABLE VI

The Effect of Artificial Compressibility Parameter on the Computation of the Eigenvalue α

n	$\gamma = 10^{12}$	$\gamma = 10^{18}$
0	$0.519991235 + 0.020832533i$	$0.519991235 + 0.020832533i$
1	$0.535248453 + 0.017227006i$	$0.535248453 + 0.017227006i$

Note. Re = 10000, $\omega = 0.5$, and $N = 20$.

and 10^{-18} using $N = 20$. The results which are shown in Table VI indicate that for moderate size matrices the round off error is insignificant.

3.4. *Temporal Stability of Poiseuille Flow in a Pipe*

There are many experimental, theoretical, and numerical papers available which are concerned with this problem. Therefore, to address the physics of the problem and do a thorough analysis of it is beyond the intent of this paper. It is reiterated that our objective is to show the numerical efficiency and the suitability of the Chebyshev collocation technique for a variety of hydrodynamic stability problems.

The linear stability of Poiseuille flow in circular pipes subjected to azimuthally varying disturbances has been attempted by Lessen *et al.* [19]. Using a shooting method, they found no instability for $n = 1$ perturbations. Two of their modes are tabulated in Table VII, along with the present calculations. The two methods agree very well. Salwen and Grosch [20] extended the work of [19] to higher n by expanding the governing equations in a set of Bessel functions and modified Bessel functions. This type of expansion is highly problem dependent, requiring a new set of functions for each new case. Salwen and Grosch found that as n increases so does the stability of the flow. This finding was confirmed by Metcalfe and Orszag [2] who used a Chebyschev tau formulation to obtain the eigenvalues. The solutions obtained by collocation reconfirms this result as shown in Table VIII. To the accuracy given by [2], the two methods generate identical results. Next the variation of the least stable mode with Reynolds number was obtained using $N = 30$. A

TABLE VII

Comparison of the Results of Lessen with Those of Chebyshev Collocation

			Lessen [19]		Present method	
n	α	Re	C_r	C_i	C_r	C_i
1	1	200	0.645	−0.129	0.64526	−0.129205
1	1	2200	—	−0.067	0.39797	−0.067709
1	1	2200	—	—	0.89663	−0.048114

TABLE VIII

Comparison of the Variation of the Imaginary Part of the Least Stable Mode as a Function of the Circumferential Wave Number, n, with $\alpha = 1$, and $\mathrm{Re} = 1000$.

	Metcalfe and Orszag [2]	Present method
n	C_i	C_i
5	−0.180604	−0.180604
7	−0.207943	−0.207943
9	−0.245645	−0.245645
21	−0.710998	−0.710998
51	−3.37925	−3.37925
101	−12.0699	−12.0699

comparison of these results with those of Salwen *et al.* [21] is given in Table IX. Again the agreement is excellent.

The value of χ in the Neurmann pressure boundary conditions on the outer wall (cf. Eq. (46)) was varied in a series of numerical experiments to ascertain its influence. In a typical case ($n = 1$, $\mathrm{Re} = 9600$, $\alpha = 1$), we found that when χ was set to zero no detectable loss in accuracy was observed in the calculated eigenvalues when compared to the results obtained using the normal momentum equation. This is not surprising since the pressure at the wall must balance the normal viscous forces and they are very small.

The question of the error which may be introduced through the Neumann boundary condition for pressure can only be addressed by comparing our results with formulations which eliminate pressure altogether. We have done this as a further test for the example case. Using 37 collocation points, we calculated

TABLE IX

A Comparison of the Variations of the Least Stable Modes with the Reynolds Number with Those of Salwen, Cotton, and Grosch [21]

Re	Mode 1	Mode 2	Mode 3	Mode 4	Mode 5	
100	0.57256 0.14714	0.55198 0.37446	0.78735 0.47946	0.66248 0.74907		Collocation
	0.57256 0.14714	0.55198 0.37446	0.78735 0.47946	0.66247 0.74907		*SCG*
1000	0.84675 0.07086	0.46914 0.09114	0.74819 0.15122	0.92730 0.15270	0.30948 0.15972	Collocation
	0.84675 0.07086	0.46916 0.09117	— —	0.92730 0.15270	0.30947 0.15973	*SCG*
9600	0.95048 0.02317	0.27684 0.04759	0.97668 0.04946	0.91886 0.04994	0.88817 0.07730	Collocation
	0.95048 0.02317	0.27681 0.04760	0.97668 0.04946	— —	— —	*SCG*

Note. $\alpha = 1$, $n = 1$. All the imaginary parts have negative sign which has been omitted for clarity.

$\omega = (0.959481397 - 0.023170795i)$ which agrees with the results of Leonard and Wray [22] to nine significant digits. Since Leonard and Wray used divergence-free expansion functions for their velocity field, pressure was eliminated from their governing equations and the question of pressure boundary condition does not arise. Consequently, the numerical tests have shown that the Neumann boundary condition for pressure, which was used in this study, produces accurate eigenvalue results. It is worth noting further that the comparisons in Sections 3.1 and 3.2 were made with Orr–Sommerfeld based calculations which did not contain pressure.

3.5. *Temporal Stability of Poiseuille Flow in a Rotating Pipe*

The stability of rotating Poiseille flow has received considerable attention in recent years. This type of flow is the simplest approximation to the trailing line vortex and at the same time is an exact solution to the Navier–Stokes equations. The mean velocity profile is of the form

$$\begin{aligned} U &= 0 \\ V &= \Omega r \\ W &= 1 - r^2, \end{aligned} \tag{50}$$

where Ω is the angular velocity of the pipe wall. The governing equations and the boundary conditions are identical to those specified in the earlier sections.

Pedley [23] produced results which were considered controversial because they indicated that the flow became unstable to asymmetric disturbances at relatively low Reynolds numbers when the pipe was rotating rapidly. His conclusion was con- [illegible] findings have been confirmed by Metcalfe and Orszag [2] after extensive calcula-

TABLE X

The Effects of Rotation on the Stability of Pipe Flow

	Metcalfe and Orszag [2]		Present method	
α	$\Omega = 0$ C_i	$\Omega = 0.1$ C_i	$\Omega = 0$ C_i	$\Omega = 0.1$ C_i
0.01	−14.683	−14.683	−14.683	−14.683
0.1	−1.4788	−1.4807	−1.4788	−1.4807
0.5	−0.34849	−0.35545	−0.34849	−0.35545
1.0	−0.27345	−0.27408	−0.27345	−0.27408
3.0	−0.19235	−0.18433	−0.19235	−0.18433
5.0	−0.17650	−0.17141	−0.17650	−0.17141
10.0	−0.1894	−0.1874	−0.1894	−0.1874

Note. Only the imaginary part is shown. Here, Re = 100, and $n = 0$.

TABLE XI

Variation of the Imaginary Part of the Least Stable Mode with Rotation

	Metcalfe and Orszag [2]	Present method
Ω	C_i	C_i
0.	−1.57781649	−1.577816485
0.0001	−1.57781648	−1.577816488
0.001	−1.57781653	−1.577816667
0.01	−1.5778346	−1.57783467
0.1	−1.5796	−1.5796
1.	−1.795	−1.795
10.	−2.29	−2.29
50.	−2.72	−2.72

Note. Re = 10, $\alpha = 1$, and $n = 0$.

tions. Here, for the sake of comparison, some of their results are reproduced. The effect of rotation on the stability of pipe flow with respect to symmetric disturbances is tabulated in Tables X and XI, along with those reported by [2]. From the above tables, it is deduced that in the case of symmetric perturbations, rotation is a stabilizing force. However, the conclusion of Pedley [23] is reconfirmed in Table XII which clearly shows the destablizing effect of the mean swirl on the pipe flow for *asymmetric* modes. Note that for the cases of Re = 2000, $\alpha = 0.1$, and Re = 130, $\alpha = 0.02$ the Chebyshev collocation results are in quantitative disagreement with those of [2]. We have tested the convergence of our results using higher values of N. Unless this disagreement is the result of a typographical error or lack of resolution in [2], in light of the excellent agreement obtained for the previous tables, it is difficult to explain the discrepancy.

TABLE XII

Determination of Some of the Unstable Modes

		Metcalfe and Orszag [2]	Present method
Re	α	C_i	C_i
200	0.001	−47.5	−47.5 (stable)
200	0.05	2.81	2.81 (unstable)
2000	0.1	−0.167	−0.07887
130	0.02	1.9761	1.9021
130	0.06	1.34	1.34
85	0.05	0.1135	0.1135

Note. $\Omega = -10$ and $n = 1$.

3.6. *Temporal Stability of a Trailing Line Vortex*

The mean velocity profile for a trailing line vortex far behind an aricraft has been obtained by Batchelor [24]. The approximate asymptotic form of the solution is

$$\begin{aligned} U &= 0 \\ V &= \frac{q}{r}[1-\exp(-r^2)] \\ W &= \exp(-r^2), \end{aligned} \tag{51}$$

where q is called the swirl parameter representing the ratio of the maximum swirl velocity to that of maximum axial velocity. Employing the above profile, Lessen and Paillet [25] have calculated the stability characteristics. Starting the solution at $r=0$ with a Frobenius series and at $r=r_{\max}$ with an asymptotic solution, they have integrated from both limits using a Taylor series expansion and matching the solutions at some intermediate radius. Lessen and Paillet [25] found that the flow stability is very much dependent on the value of q and for values slightly greater than 1.5, all unstable modes are highly damped and stabilized.

Since r varies between zero and infinity, an algebraic transformation given by Malik *et al.* [26] is employed in the form

$$r = a\frac{1+\xi}{b-\xi}, \tag{52}$$

where a and b are constants. For any arbitrary value of a, b is uniquely determined by

$$b = 1 + \frac{2a}{r_{\max}}. \tag{53}$$

It should be noted here that parameter a is very significant in that the above transformation concentrates at least half of the collocation points between $r=0$ and $r=a$. Now, a closer look at (51) would reveal that for $r>3$ the axial velocity is essentially zero and the azimuthal velocity approaches q/r, which is a potential vortex. Therefore, the value of a was set to 3 (incidentially, this value corresponds to the $r_{\max}$ of Lessen and Paillet [25], where they have started their asymptotic solution) and $r_{\max}=100$. A test was performed to make sure that the far field conditions where perturbations are set to zero applies at this finite value of $r_{\max}$. That is, the value of $r_{\max}$ was set equal to 500 and then 1000 while keeping N constant and the movement of the eigenvalues was observed. Next, fixing $r_{\max}$ at 1000, the number of collocation points was increased gradually until five or six digit convergence was obtained. The above test revealed that for a very moderate number of collocation points, the $r_{\max}=100$ was sufficient and the desired eigenvalues had already converged to four or five significant digits.

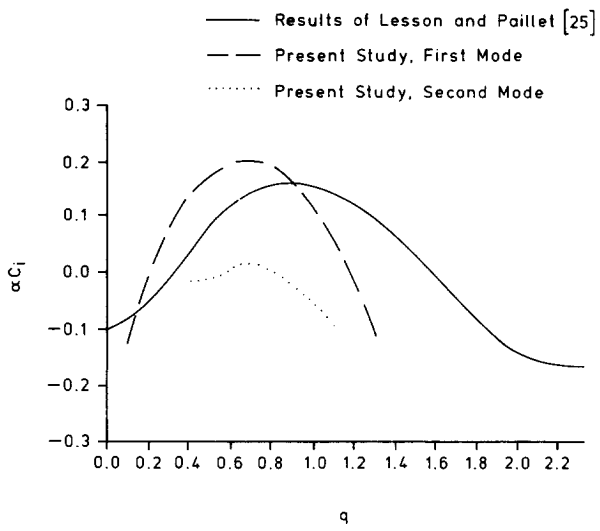

FIG. 1. Variation of growth rate αC_i, with swirl parameter q, for temporal stability of a trailing line vortex (Re = 141.4, $\alpha = 1.34$, $n = -2$).

Figure 1 demonstrates the variation of αC_i as a function of q along with the curve computed by Lessen and Paillet [25]. Although both methods show similar trends, the Chebyshev collocation results indicate the presence of a second instability mode which was not given by [25]. Also the entire growth rate curve computed by the collocation for the mode given by [25] is shifted to the left with higher maximum growth rate and a narrower region (smaller range of q) of instability. The above differences created the suspicion that transformation (52) may not have been suitable for the present problem and could have introduced errors in imposition of the far field boundary conditions. Therefore, a new coordinate stretching which has been given by Streett and Hussaini [27] was employed. That transformation is

$$r = \frac{[1 + b\exp(-a)]\, r_{\max}}{[1 + b\exp(-a((1-\xi)/2))]} \left(\frac{1-\xi}{2}\right), \tag{54}$$

where a and b are constants and are assigned values in the range of 2 to 3 and 5 to 50, respectively. This mapping clusters the cell points near the two boundaries and has somewhat different characteristics than (52). A test was conducted using this transformation with $r_{\max}$ fixed at 1000. The value of N was increased gradually until the eigenvalues were converged to six or seven significant digits. It was found that both transformations (52) and (54) gave identical results. Because of the different nature of these two mappings, the above findings support the correctness of concentrating more computational points near the centerline boundary and highly stretching the points in the outer part of the flow. With regard to the discrepancies between this work and [25], the possibility exists that their starting asymptotic

solution at $r_{max} = 3$ is not fully valid and raises the question of whether their integration should have started at a larger value of r_{max}.

Before concluding this last section, we should mention that it is possible to reduce the governing equations (1)–(4) to a system which consists of a fourth-order equation plus a second-order equation. In the temporal formulation case, the new system would require one-fourth as much computer storage, but for the spatial formulation (which is the desired and intended form of calculation), the memory savings is not very substantial. In fact, the present seven equations model would only be reduced to a six equations model with the added complexity of dealing with higher order operators (more matrix multiplications to generate higher order operations) and more complex equations.

4. Conclusions

A Chebyshev spectral collocation method for studying the temporal and spatial stability of incompressible swirling flows has been developed. The primitive variable formulation of the governing equations has been used in the present study. This is in contrast with the standard approach of reducing the governing equations to a set of a fourth-order equation and a second-order equation. While the present formulation requires somewhat higher computer storage for eigenvalue calculation using the QZ algorithm, it is easily adaptable to various flow situations and is also suitable for compressible flows. The method has been applied to various temporal and spatial stability problems including flow through a pipe and an annulus, rotating pipe flow, and a trailing line vortex. While our results are in general agreement with the results of Bridges and Morris [4], Orszag [1], Garg and Rouleau [18], Lessen, Sadler and Liu [19], Melcalfe and Orszag [2], Salwen, Cotton, and Grosch [21], some quantitative disagreement with the results of Lessen and Paillet [25] for a trailing line vortex was found.

Acknowledgments

One of the authors (M.R.K.) would like to acknowledge several useful discussions with Professor C. E. Grosch of Old Dominion University, Professor D. Gottlieb of Brown University, and Dr. M. Y. Hussaini of ICASE at NASA Langley Research Center. Research of the first and the third authors was supported under NASA Grant NAG-1-530 and that of the second author under Contract NAS1-18240.

References

1. S. A. Orszag, *J. Fluid Mech.* **50**, 689 (1971).
2. R. W. Metcalfe and S. A. Orszag, Flow Research Report No. 25, 1973 (unpublished).
3. A. Zebib, *J. Comput. Phys.* **53**, 443 (1984).
4. T. J. Bridges and P. J. Morris, *J. Comput. Phys.* **55**, 437 (1984).

5. L. N. HOWARD AND A. S. GUPTA, *J. Fluid Mech.* **14**, 463 (1962).
6. T. HERBERT, AIAA Paper 83-1759, 1983 (unpublished).
7. P. R. SPALART, NASA TM 88222, 1986 (unpublished).
8. C. DUP. DONALDSON AND R. D. SULLIVAN, Aeronautical Research Associates of Princeton, AFOSR TN 60-1227, 1960 (unpublished).
9. G. N. ADAMS AND D. C. GILMORE, *Canad. Aeronaut. Space J.* **18**, 159 (1972).
10. O. LEUCHTER AND J. L. SOLIGNAC, ONERA, TP No. 1983-107, 1983 (unpublished).
11. J. A. H. GRAHAM AND B. G. NEWMAN, "Turbulent Trailing Vortex with Central Jet and Wake," The Ninth Congress of the International Council of the Aeronautical Sciences, ICAS No. 74-40, 1974 (unpublished).
12. G. K. BATCHELOR AND A. E. GILL, *J. Fluid Mech.* **14**, 34 (1962).
13. D. GOTTLIEB AND S. A. ORSZAG, *Numerical Analysis of Spectral Methods: Theory and Applications* (Soc. Indus. & Appl. Math., Philadelphia 1977).
14. M. Y. HUSSAINI, C. L. STREETT, AND T. A. ZANG, in *Transactions of the First Army Conference on Applied Mathematics and Computing*, ARO *Report* 84-1, 1984 (unpublished).
15. D. GOTTLIEB, M. Y. HUSSAINI, AND S. A. ORSZAG, "Theory and Application of Spectral Methods,"
16. M. R. MALIK AND D. I. A. POLL, *AIAA J.* **23**, 1362 (1985).
17. S. A. ORSZAG AND M. ISRAELI, *Ann. Rev. Fluid Mech.* **6**, 281 (1974).
18. V. K. GARG AND W. T. ROULEAU, *J. Fluid Mech.* **54**, 113 (1972).
19. M. LESSEN, S. SADLER, AND T. LIU, *Phys. Fluids* **11**, 1404 (1968).
20. H. SALWEN AND C. E. GROSCH, *J. Fluid Mech.* **54**, 93 (1972).
21. H. SALWEN, F. W. COTTON, AND C. E. GROSCH, *J. Fluid Mech.* **98**, 273 (1980).
22. A. LEONARD AND A. WRAY, in *Proceedings, Eights International Conference on Numerical Methods in Fluid Dynamics, Aachen, West Germany, 1982*, edited by E. Krause (Springer-Verlag, Berlin, 1982), p. 335.
23. T. J. PEDLEY, *J. Fluid Mech.* **35**, 97 (1969).
24. G. K. BATCHELOR, *J. Fluid Mech.* **20**, 645 (1964).
25. M. LESSEN AND F. PAILLET, *J. Fluid Mech.* **65**, 769 (1974).
26. M. R. MALIK, T. A. ZANG, AND M. Y. HUSSAINI, *J. Comput. Phys.* **61**, 64 (1985).
27. C. L. STREETT AND M. Y. HUSSAINI, "Finite Length Taylor Couette Flow," in *Stability of Time Dependent Spatially Varying Flows*, edited by D. L. Dwoyer and M. Y. Hussaini (Springer-Verlag, New York, 1987), p. 312.